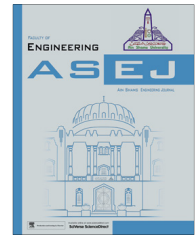




Ain Shams University

Ain Shams Engineering Journal

www.elsevier.com/locate/asej  
www.sciencedirect.com



ENGINEERING PHYSICS AND MATHEMATICS

# The influence of thermophoretic particle deposition on fully developed MHD mixed convective flow in a vertical channel with thermal-diffusion and diffusion-thermo effects

D. Lourdu Immaculate <sup>a</sup>, R. Muthuraj <sup>b,\*</sup>, R.K. Selvi <sup>b</sup>, S. Srinivas <sup>c</sup>,  
Anant Kant Shukla <sup>d</sup>

<sup>a</sup> Department of Mathematics, The American College, Madurai 625 002, India

<sup>b</sup> Department of Mathematics, PSNACET, Dindigul 624622, India

<sup>c</sup> School of Advanced Sciences, VIT University, Vellore 632 014, India

<sup>d</sup> Department of Mathematics, Amrita School of Engineering, Amrita Vishwa Vidyapeetham, Amritanagar P.O., Coimbatore 641112, India

Received 11 August 2014; revised 20 October 2014; accepted 18 November 2014

## KEYWORDS

MHD;  
Homotopy analysis method;  
Thermophoretic deposition;  
Soret number;  
Dufour number

**Abstract** The present paper deals with the influence of thermophoretic particle deposition on the MHD mixed convective heat and mass transfer flow in a vertical channel in the presence of radiative heat flux with thermal-diffusion and diffusion-thermo effects. The resulting nonlinear coupled equations are solved under appropriate boundary conditions using the homotopy analysis method. The influence of involved parameters on heat and mass transfer characteristics of the fluid flow is presented graphically. It is noted that fluid velocity is an increasing function of radiation parameter, Dufour number, Buoyancy ratio parameter and mixed convection parameter whereas the magnetic parameter, thermophoresis constant, Soret number and Schmidt number lead to suppress the velocity. The fluid temperature increases with increasing radiation parameter and Dufour number. The convergence of homotopy analysis method (HAM) solutions is discussed and a good agreement is found between the analytical and the numerical solution.

© 2014 Faculty of Engineering, Ain Shams University. Production and hosting by Elsevier B.V. This is an open access article under the CC BY-NC-ND license (<http://creativecommons.org/licenses/by-nc-nd/4.0/>).

\* Corresponding author. Tel.: +91 451 2554032.

E-mail address: [dr.ramamoorthyathuraj@gmail.com](mailto:dr.ramamoorthyathuraj@gmail.com) (R. Muthuraj).

Peer review under responsibility of Ain Shams University.



Production and hosting by Elsevier

## 1. Introduction

Mixed convection flow in a vertical channel has been the subject of many investigations due to its important applications in industrial and engineering processes such as cooling of electronic equipment, heat exchangers, chemical processing equipments and others. Also, mixed convection flow in a vertical

<http://dx.doi.org/10.1016/j.asej.2014.11.010>

2090-4479 © 2014 Faculty of Engineering, Ain Shams University. Production and hosting by Elsevier B.V.

This is an open access article under the CC BY-NC-ND license (<http://creativecommons.org/licenses/by-nc-nd/4.0/>).

Please cite this article in press as: Lourdu Immaculate D et al., The influence of thermophoretic particle deposition on fully developed MHD mixed convective flow in a vertical channel with thermal-diffusion and diffusion-thermo effects, Ain Shams Eng J (2015), <http://dx.doi.org/10.1016/j.asej.2014.11.010>

**Nomenclature**

$B$	buoyancy ratio parameter	$S_c$	Schmidt number
$B_0$	transverse magnetic field	Sh	Sherwood number
$C$	concentration of the fluid	$S_r$	Soret number
$C_1, C_2$	wall concentrations	$T$	temperature of the fluid
$c_p$	specific heat at constant pressure	$T_1, T_2$	wall temperatures
$c_s$	concentration susceptibility	$\bar{T}$	mean value of $T_1$ and $T_2$
$D_u$	Dufour number	$u$	fluid velocity
$D_m$	coefficient of mass diffusivity	$U_0$	entrance velocity
$g$	Gravitational force	$v$	thermophoretic deposition velocity
$G_r$	Grashof number	$V_T$	non-dimensional thermophoretic velocity
$G_R$	mixed convection parameter		
$K$	thermal conductivity		
$k$	non-dimensional thermophoretic coefficient which depends on Knudsen number	<i>Greek symbols</i>	
$k_T$	thermal diffusion ratio	$\theta$	non-dimensional fluid temperature
$L$	width of the channel	$\phi$	nondimensional fluid concentration
$M$	magnetic parameter	$\beta_c$	coefficient of volume expansion
$N$	radiation parameter	$\beta_T$	coefficient of thermal expansion
$N_t$	non-dimensional parameter	$\mu$	dynamic viscosity
$Nu$	Nusselt number	$\sigma$	electrical conductivity
$P$	pressure	$\rho$	fluid density
$P_r$	Prandtl number	$\nu$	kinematic viscosity
$q$	radiative heat flux	$\alpha$	non-dimensional pressure gradient
Re	Reynolds number	$\alpha_1^2$	mean absorption coefficient
		$\tau$	skin friction

channel in the presence of a transverse magnetic field is of special technical significance because of its industrial applications such as geothermal reservoirs, cooling of nuclear reactors, petroleum reservoirs and so on. This type of problem arises in electronic packages, microelectronic devices during their operations also. Excellent reviews of the mixed convection hydromagnetic flows in vertical channel have been presented by many authors [1–5]. Later, Srinivas and Muthuraj [6] have examined the problem of MHD flow in a vertical wavy porous space in the presence of a temperature-dependent heat source with slip-flow boundary condition. They have also examined the effects of chemical reaction and space porosity on MHD mixed convective peristaltic flow in a vertical asymmetric channel [7]. Fully developed mixed convection flow in a vertical channel filled with nanofluids was discussed analytically by Xu and Pop [8]. Rashidi et al. [9] have analyzed the effects of partial slip and thermal-diffusion and diffusion-thermo on Steady MHD Convective Flow due to a Rotating Disk.

Thermophoresis is a phenomenon observed in mixtures of mobile particles where the different particle types exhibit different responses to the force of a temperature gradient. The term thermophoresis most often applies to aerosol mixtures, but it may commonly refer to the phenomenon in all phases of matter. This thermophoresis process has gained importance for many engineering applications and is utilized in air-cleaning devices to remove submicron- and micron-sized particles from gas streams ([10–21]). In view of these applications, a theoretical analysis for thermophoretic transport of small particles through a fully developed laminar, mixed convection flow in a parallel vertical channel was presented by Grosan et al. (see Ref. [16] and several references therein). Later, thermophoretic transport in the steady fully developed mixed

convection flow in a parallel-plate vertical channel with differentially heated isothermal walls was studied by Magyari [17]. Mahdy and Hady [18] have analyzed the effects of thermophoretic particle deposition on the free convective flow over a vertical flat plate embedded in a non-Newtonian fluid-saturated porous medium in the presence of a magnetic field. The effect of surface mass transfer on MHD mixed convection flow past a heated vertical flat permeable surface in the presence of thermophoresis, radiative heat flux and heat source/sink using similarity transformation was studied by Singh et al. [19]. Free convection thermophoretic hydromagnetic flow over a radiate isothermal inclined plate with heat source/sink effect using shooting method were presented by Noor et al. [20]. More recently, Guha and Samanta [21] have investigated the effects of thermophoresis and transverse magnetic field on aerosol particle transport and deposition onto a horizontal plate in the presence of a natural convective flow. To the best of our knowledge, no attempt has been made to analyze the influences of thermophoresis deposition, thermal-diffusion and diffusion-thermo on hydromagnetic flow in a vertical channel with asymmetric wall temperatures. Motivated by previous studies, a mathematical model is to be presented to understand the combined effects of thermophoresis deposition, thermal-diffusion and diffusion-thermo on MHD flow in a vertical channel with heat and mass transfer. Such problems are important in flow analysis for the understanding of flow, heat and mass transfer characteristics. Analytic solutions for the velocity, heat and mass transfer components are obtained using a powerful, easy to use technique, namely the homotopy analysis method (HAM). It is worth mentioning that the HAM is a promising tool for solving non-linear problems ([22–35]). Heat and mass transfer characteristics of the fluid flow for

various values of the pertinent parameters have been reported graphically. This paper is organized as follows: The problem is formulated in Section 2. Section 3 comprises the solutions of the problem. Convergence and residual error analysis of HAM solution are presented in Section 4. Results and discussion are given in Section 5. Section 6 contains final remarks.

## 2. Formulation of the problem

The geometry under consideration illustrated in Fig. 1, which consists of two infinite vertical channel walls maintained at constant temperatures and concentrations  $T_1, T_2$  ( $T_2 > T_1$ ) and  $C_1, C_2$  ( $C_2 > C_1$ ) respectively. A fluid rises in the channel driven by buoyancy forces. We consider the fluids to be an incompressible viscous fluid and the flow is steady, laminar and fully developed. A uniform magnetic field is applied normal to the flow direction. The governing equations for this problem are based on the balance laws of mass, linear momentum, energy and concentration modified to account for the presence of the magnetic field. These can be written as (Ref. [16])

$$\mu \frac{d^2 u}{dy^2} + \rho g [\beta_T (T - T_1) + \beta_c (C - C_1)] - \sigma B_0^2 u = \frac{dP}{dx} \quad (1)$$

$$\frac{K}{\rho C_p} \frac{d^2 T}{dy^2} - \frac{1}{\rho C_p} \frac{dq}{dy} + \frac{D_m K_T}{C_p C_s} \frac{d^2 C}{dy^2} = 0 \quad (2)$$

$$D_m \frac{d^2 C}{dy^2} + \frac{D_m K_T}{\bar{T}} \frac{d^2 T}{dy^2} = \frac{d(Cv_T)}{dy} \quad (3)$$

The boundary conditions of the problem are,

$$u = 0, \quad T = T_1, \quad C = C_1 \quad \text{at } y = -L \quad (4)$$

$$u = 0, \quad T = T_2, \quad C = C_2 \quad \text{at } y = L \quad (5)$$

Further,  $v_T$  is the thermophoretic deposition velocity in the  $y$ -direction and we assume that  $v_T$  has the form:

$$v_T = -k \frac{v}{T} \frac{dT}{dy} \quad (6)$$

where  $u$  is the velocity component,  $P$  is the pressure,  $\mu$  is the dynamic viscosity,  $\rho$  is the density,  $B_0$  is the transverse magnetic field,  $\sigma$  is the coefficient of electric conductivity,  $D_m$  is the coefficient of mass diffusivity,  $T$  is the dimensional temperature,  $C$  is the dimensional concentration,  $C_p$  is the specific

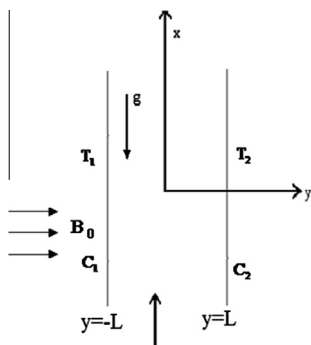


Figure 1 Flow Geometry of the problem.

heat,  $T_1$  and  $T_2$  are the wall temperatures,  $\bar{T}$  is the mean value of  $T_1$  and  $T_2$ ,  $K$  is the thermal conductivity of the fluid,  $k_T$  is the thermal diffusion ratio,  $C_1$  and  $C_2$  are the wall concentrations. We define the non-dimensional variables as,

$$y^* = \frac{y}{L}, \quad u^* = \frac{u}{U_0}, \quad \theta = \frac{T - T_1}{T_2 - T_1}, \quad \phi = \frac{C - C_1}{C_2 - C_1},$$

$$V_T = \frac{Lv_T}{v}, \quad \alpha = \frac{L^2}{\mu U_0} \frac{dP}{dx}, \quad \frac{dq}{dy} = 4\alpha_1^2 (T_1 - T) \quad (7)$$

Substituting Eq. (7) into the Eqs. (1)–(6), we get (dropping asterisks)

$$\frac{d^2 u}{dy^2} + \frac{G_r}{Re} [\theta + B\phi] - M^2 u = \alpha \quad (8)$$

$$\frac{d^2 \theta}{dy^2} + D_u P_r \frac{d^2 \phi}{dy^2} + N\theta = 0 \quad (9)$$

$$(N_t + \theta)^2 \frac{d^2 \phi}{dy^2} + S_r S_c (N_t + \theta)^2 \frac{d^2 \theta}{dy^2} + k S_c (N_t + \theta) \frac{d\theta}{dy} \frac{d\phi}{dy}$$

$$+ \left[ S_c k (N_t + \theta) \frac{d^2 \theta}{dy^2} - S_c k \left( \frac{d\theta}{dy} \right)^2 \right] (\phi + \beta_1) = 0 \quad (10)$$

With the boundary conditions

$$u = 0, \quad \theta = 0, \quad \phi = 0 \quad \text{at } y = -1 \quad (11)$$

$$u = 0, \quad \theta = 1, \quad \phi = 1 \quad \text{at } y = 1 \quad (12)$$

The non-dimensional thermophoretic velocity  $V_T$  can be expressed as

$$V_T = -\frac{k}{N_t + \theta} \frac{d\theta}{dY} \quad (13)$$

where  $N_t = \frac{T_1}{T_2 - T_1}$  and  $\beta_1 = \frac{C_1}{C_2 - C_1}$  are the non-dimensional constants,  $G_r = \frac{g\beta_T(T_2 - T_1)L^3}{\nu^2}$  is the Grashof number,  $Re = \frac{\rho U_0 L}{\mu}$  is the Reynolds number,  $G_R = \frac{G_r}{Re}$  is the mixed convection parameter,  $B = \frac{\beta_c(C_2 - C_1)}{\beta_T(T_2 - T_1)}$  is the Buoyancy ratio parameter,  $M^2 = \frac{\sigma B_0^2 L^2}{\rho \nu}$  is the Hartmann number,  $\nu = \frac{\mu}{\rho}$  is the kinematic viscosity,  $D_u = \frac{D_m k_T (C_2 - C_1)}{\nu C_p C_s (T_2 - T_1)}$  is the Dufour number,  $P_r = \frac{\mu C_p}{K}$  is the Prandtl number,  $N = \frac{4\alpha_1^2 L^2}{K}$  is the radiation parameter,  $\frac{dq}{dy} = 4\alpha_1^2 (T_1 - T)$  is the radiative heat flux,  $\alpha_1^2$  is the mean absorption coefficient,  $S_c = \frac{\nu}{D_m}$  is the Schmidt number,  $S_r = \frac{D_m K_T (T_2 - T_1)}{\bar{T} (C_2 - C_1)}$  is the Soret number,  $V_T$  is the non-dimensional thermophoretic velocity,  $k$  is the non-dimensional thermophoretic coefficient which depends on the Knudsen number ( $Kn \gg 1$ ).

## 3. Solution of the problem

For complete description of the homotopy analysis method (HAM) the reader is referred to [22,23]. We choose the initial guesses and the auxiliary linear operators for the problem stated above in the following forms:

$$u_0(y) = 0 \quad \theta_0(y) = \frac{1+y}{2} \quad \phi_0(y) = \frac{1+y}{2} \quad (14)$$

$$L_1(u) = u'' \quad L_2(\theta) = \theta'' \quad L_3(\phi) = \phi'' \quad (15)$$

with

$$L_1(c_1y + c_2) = 0, \quad L_2(c_3y + c_4) = 0 \quad \& \quad L_3(c_5y + c_6) = 0.$$

where  $c_i(i = 1, 2, 3, 4, 5, 6)$  are constants and prime denotes the derivative with respect to  $y$ .

### 3.1. Zeroth-order approximation

Let  $\varphi \in [0, 1]$  be an embedding parameter and  $h$  be the auxiliary non-zero parameter. We construct the following zero-order deformation equations.

$$(1 - \varphi)L_1[\hat{u}(y, \varphi) - u_0(y)] = \varphi h N_1[\hat{u}(y, \varphi), \hat{\theta}(y, \varphi), \hat{\phi}(y, \varphi)]$$

$$\hat{u}(-1, \varphi) = 0, \hat{u}(1, \varphi) = 0 \tag{16}$$

$$(1 - \varphi)L_2[\hat{\theta}(y, \varphi) - \theta_0(y)] = \varphi h N_2[\hat{\theta}(y, \varphi), \hat{\phi}(y, \varphi)]$$

$$\hat{\theta}(-1, \varphi) = 0, \hat{\theta}(1, \varphi) = 1 \tag{17}$$

$$(1 - \varphi)L_3[\hat{\phi}(y, \varphi) - \phi_0(y)] = \varphi h N_3[\hat{\theta}(y, \varphi), \hat{\phi}(y, \varphi)]$$

$$\hat{\phi}(-1, \varphi) = 0, \hat{\phi}(1, \varphi) = 1 \tag{18}$$

where,

$$N_1[\hat{u}(y, \varphi), \hat{\theta}(y, \varphi), \hat{\phi}(y, \varphi)] = \frac{\partial^2 \hat{u}(y, \varphi)}{\partial y^2} + G_R[\hat{\theta}(y, \varphi) + B\hat{\phi}(y, \varphi)] - M^2 \hat{u}(y, \varphi) - \alpha \tag{19}$$

$$N_2[\hat{\theta}(y, \varphi), \hat{\phi}(y, \varphi)] = \frac{\partial^2 \hat{\theta}(y, \varphi)}{\partial y^2} + D_u P_r \frac{\partial^2 \hat{\phi}(y, \varphi)}{\partial y^2} + N\hat{\theta}(y, \varphi) \tag{20}$$

$$N_3[\hat{\theta}(y, \varphi), \hat{\phi}(y, \varphi)] = (N_t + \hat{\theta}(y, \varphi))^2 \frac{\partial^2 \hat{\phi}(y, \varphi)}{\partial y^2} + S_r S_c (N_t + \hat{\theta}(y, \varphi))^2 \frac{\partial^2 \hat{\theta}(y, \varphi)}{\partial y^2} + k S_c (N_t + \hat{\theta}(y, \varphi)) \frac{\partial \hat{\theta}(y, \varphi)}{\partial y} \frac{\partial \hat{\phi}(y, \varphi)}{\partial y} + \left[ S_c k (N_t + \hat{\theta}(y, \varphi)) \frac{\partial^2 \hat{\theta}(y, \varphi)}{\partial y^2} - S_c k \left( \frac{\partial \hat{\theta}(y, \varphi)}{\partial y} \right)^2 \right] \times (\hat{\phi}(y, \varphi) + \beta_1) \tag{21}$$

For  $\varphi = 0$  and  $\varphi = 1$ , we have

$$\hat{u}(y, 0) = u_0(y) \quad \hat{u}(y, 1) = u(y) \tag{22}$$

$$\hat{\theta}(y, 0) = \theta_0(y) \quad \hat{\theta}(y, 1) = \theta(y) \tag{23}$$

$$\hat{\phi}(y, 0) = \phi_0(y) \quad \hat{\phi}(y, 1) = \phi(y) \tag{24}$$

when  $\varphi$  increases from 0 to 1, then  $\hat{u}(y, \varphi)$ ,  $\hat{\theta}(y, \varphi)$ ,  $\hat{\phi}(y, \varphi)$  vary from initial guess  $u_0(y)$ ,  $\theta_0(y)$ ,  $\phi_0(y)$  to the approximate analytical solution  $u(y)$ ,  $\theta(y)$ ,  $\phi(y)$ .

By Taylor's theorem the series  $\hat{u}(y, \varphi)$ ,  $\hat{\theta}(y, \varphi)$ ,  $\hat{\phi}(y, \varphi)$  can be expressed as a power series of  $\varphi$  as follows,

$$\hat{u}(y, \varphi) = u_0(y) + \sum_{m=1}^{\infty} u_m(y) \varphi^m, \quad u_m(y) = \frac{1}{m!} \left. \frac{\partial^m \hat{u}(y, \varphi)}{\partial \varphi^m} \right|_{\varphi=0} \tag{25}$$

$$\hat{\theta}(y, \varphi) = \theta_0(y) + \sum_{m=1}^{\infty} \theta_m(y) \varphi^m, \quad \theta_m(y) = \frac{1}{m!} \left. \frac{\partial^m \hat{\theta}(y, \varphi)}{\partial \varphi^m} \right|_{\varphi=0} \tag{26}$$

$$\hat{\phi}(y, \varphi) = \phi_0(y) + \sum_{m=1}^{\infty} \phi_m(y) \varphi^m, \quad \phi_m(y) = \frac{1}{m!} \left. \frac{\partial^m \hat{\phi}(y, \varphi)}{\partial \varphi^m} \right|_{\varphi=0} \tag{27}$$

In which  $h$  is chosen in such a way that these series are convergent at  $\varphi = 1$ , therefore we have from Eqs. (25)–(27),

$$u(y) = u_0(y) + \sum_{m=1}^{\infty} u_m(y), \quad \theta(y) = \theta_0(y) + \sum_{m=1}^{\infty} \theta_m(y),$$

$$\phi(y) = \phi_0(y) + \sum_{m=1}^{\infty} \phi_m(y) \tag{28}$$

### 3.2. The $m$ -th order deformation equations

Differentiating the zeroth-order approximation Eqs. (16)–(18)  $m$ -times with respect to  $\varphi$  and then dividing them by  $m!$  and finally setting  $\varphi = 0$ , we obtain the following  $m$ -th order deformation equations:

$$L_1[u_m(y) - \chi_m u_{m-1}(y)] = h R_m^u(y) \tag{29}$$

$$L_2[\theta_m(y) - \chi_m \theta_{m-1}(y)] = h R_m^\theta(y) \tag{30}$$

$$L_3[\phi_m(y) - \chi_m \phi_{m-1}(y)] = h R_m^\phi(y) \tag{31}$$

together with conditions

$$u_m(-1) = 0 \quad u_m(1) = 0 \tag{32}$$

$$\theta_m(-1) = 0 \quad \theta_m(1) = 0 \tag{33}$$

$$\phi_m(-1) = 0 \quad \phi_m(1) = 0 \tag{34}$$

where,

$$R_m^u(y) = u''_{m-1} + G_R(\theta_{m-1} + B\phi_{m-1}) - M^2 u_{m-1} - \alpha(1 - \chi_m) \tag{35}$$

$$R_m^\theta(y) = \theta''_{m-1} + D_u P_r \phi''_{m-1} + N\theta_{m-1} \tag{36}$$

$$R_m^\phi(y) = N_t \phi''_{m-1} + \sum_{k=0}^{m-1} \phi''_{m-1-k} \sum_{l=0}^k \theta_k \theta_{k-l} + 2N_t \sum_{k=0}^{m-1} \theta_{m-1-k} \phi''_k + S_c S_r \left[ N_t^2 \theta''_{m-1} + \sum_{k=0}^{m-1} \theta''_{m-1-k} \sum_{l=0}^k \theta_k \theta_{k-l} + 2N_t \sum_{k=0}^{m-1} \theta_k \theta''_{m-1-k} \right] + k S_c \left[ N_t \sum_{k=0}^{m-1} \theta'_{m-1-k} \phi'_k + \sum_{k=0}^{m-1} \phi'_{m-1-k} \sum_{l=0}^k \theta_l \theta'_{k-l} \right] + k S_c \left[ N_t \sum_{k=0}^{m-1} \phi_{m-1-k} \theta''_k + \sum_{k=0}^{m-1} \phi_{m-1-k} \sum_{l=0}^k \theta_l \theta'_{k-l} - \sum_{k=0}^{m-1} \phi_{m-1-k} \sum_{l=0}^k \theta'_l \theta'_{k-l} \right] + k S_c \beta_1 \left[ N_t \theta''_{m-1} + \sum_{k=0}^{m-1} \theta_k \theta''_{m-1-k} \right] - k S_c \beta_1 \left[ \sum_{k=0}^{m-1} \theta'_k \theta'_{m-1-k} \right] \tag{37}$$

where,

$$\chi_m = \begin{cases} 0; & \text{for } m = 1 \\ 1; & \text{for } m \neq 1 \end{cases} \tag{38}$$

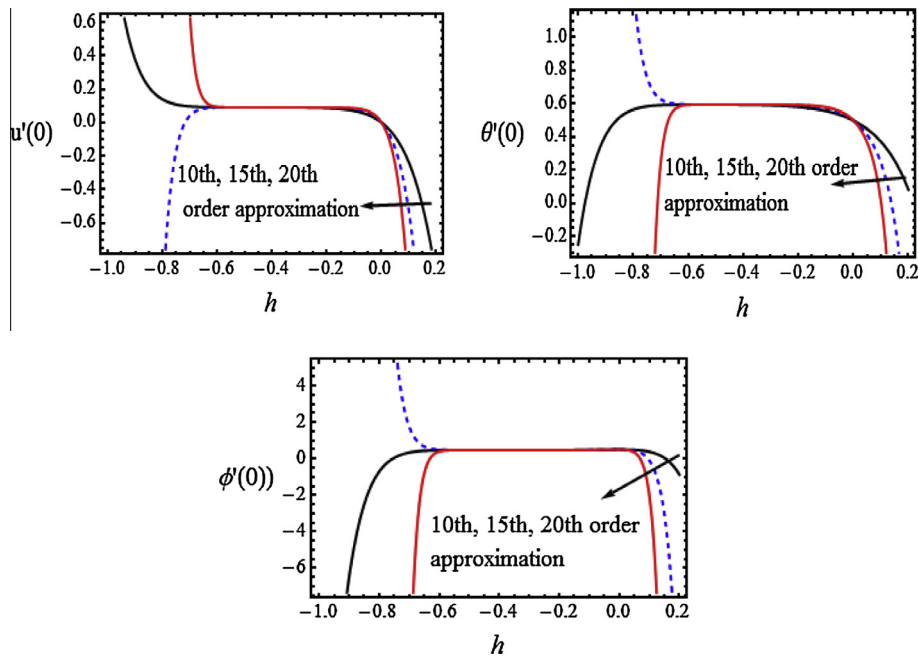


**Figure 2**  $h$ -curves for velocity, temperature and concentration for different order of approximations.

The physical quantities of interest in this problem are the skin friction, the Nusselt number and Sherwood number, which are defined as

$$\tau = \left(\frac{du}{dy}\right)_{y=\pm 1}; \quad \text{Nu} = -\left(\frac{d\theta}{dy}\right)_{y=\pm 1}; \quad \text{and}$$

$$\text{Sh} = -\left(\frac{d\phi}{dy}\right)_{y=\pm 1} \quad \text{respectively.} \quad (39)$$

#### 4. Convergence and the residual error of HAM solution

The analytic expressions given in Eq. (28) contain the auxiliary parameter  $h$ . The convergence and rate of approximation for the HAM solution depends on the value of auxiliary parameter ‘ $h$ ’ strongly. To see the range of admissible values of  $h$  the  $h$ -curves are plotted in Fig. 2.

**Table 1** The square residual error and the average square residual error for the optimal  $h$  at different order of HAM approximations. ( $S_r = 0.5, S_c = 0.5, k = 0.1, B = 0.5, P_r = 0.71, M = 2, D_u = 0.1, G_R = 1$ ).

Optimal $h$		5th order			
		$\int_{y=-1}^1 E_1^2 dy$	$\int_{y=-1}^1 E_2^2 dy$	$\int_{y=-1}^1 E_3^2 dy$	$A_m$
-0.45	$N = 0$	$2.96254 \times 10^{-4}$	$2.95283 \times 10^{-9}$	$3.49079 \times 10^{-7}$	$9.886 \times 10^{-5}$
-0.43	$M = 2$	$1.15042 \times 10^{-3}$	$2.55995 \times 10^{-2}$	$6.88199 \times 10^{-3}$	$1.12106 \times 10^{-2}$
-0.42	$S_c = 0.78$	$1.17056 \times 10^{-3}$	$2.96293 \times 10^{-2}$	$1.93553 \times 10^{-2}$	$1.67184 \times 10^{-2}$
-0.41	$K = 0.3$	$1.43806 \times 10^{-3}$	$3.6207 \times 10^{-2}$	$3.28695 \times 10^{-2}$	$2.16428 \times 10^{-2}$
-0.43	$D_u = 0.5$	$1.46737 \times 10^{-3}$	$4.06148 \times 10^{-2}$	$1.00291 \times 10^{-2}$	$1.73704 \times 10^{-2}$
		10th order			
		$\int_{y=-1}^1 E_1^2 dy$	$\int_{y=-1}^1 E_2^2 dy$	$\int_{y=-1}^1 E_3^2 dy$	$A_m$
-0.45	$N = 0$	$5.48811 \times 10^{-7}$	$3.62745 \times 10^{-11}$	$7.05032 \times 10^{-8}$	$2.0645 \times 10^{-7}$
-0.43	$M = 2$	$4.25106 \times 10^{-5}$	$1.42923 \times 10^{-3}$	$2.56242 \times 10^{-3}$	$1.34472 \times 10^{-3}$
-0.42	$S_c = 0.78$	$4.65224 \times 10^{-5}$	$1.90276 \times 10^{-3}$	$8.37047 \times 10^{-3}$	$3.43992 \times 10^{-3}$
-0.41	$K = 0.3$	$5.83831 \times 10^{-5}$	$2.00292 \times 10^{-3}$	$2.60088 \times 10^{-2}$	$9.35669 \times 10^{-3}$
-0.43	$D_u = 0.5$	$9.85295 \times 10^{-5}$	$3.71009 \times 10^{-3}$	$2.99627 \times 10^{-3}$	$2.2683 \times 10^{-3}$
		15th order			
		$\int_{y=-1}^1 E_1^2 dy$	$\int_{y=-1}^1 E_2^2 dy$	$\int_{y=-1}^1 E_3^2 dy$	$A_m$
-0.45	$N = 0$	$1.14565 \times 10^{-9}$	$1.59454 \times 10^{-12}$	$1.32751 \times 10^{-8}$	$4.80744 \times 10^{-9}$
-0.43	$M = 2$	$2.49462 \times 10^{-6}$	$8.2153 \times 10^{-5}$	$2.76652 \times 10^{-3}$	$9.50388 \times 10^{-4}$
-0.42	$S_c = 0.78$	$3.19418 \times 10^{-6}$	$1.24807 \times 10^{-4}$	$8.66284 \times 10^{-3}$	$2.93028 \times 10^{-3}$
-0.41	$K = 0.3$	$4.02765 \times 10^{-6}$	$1.34729 \times 10^{-4}$	$2.65164 \times 10^{-2}$	$8.88506 \times 10^{-3}$
-0.43	$D_u = 0.5$	$9.12656 \times 10^{-6}$	$3.2609 \times 10^{-4}$	$3.34668 \times 10^{-3}$	$1.2273 \times 10^{-3}$

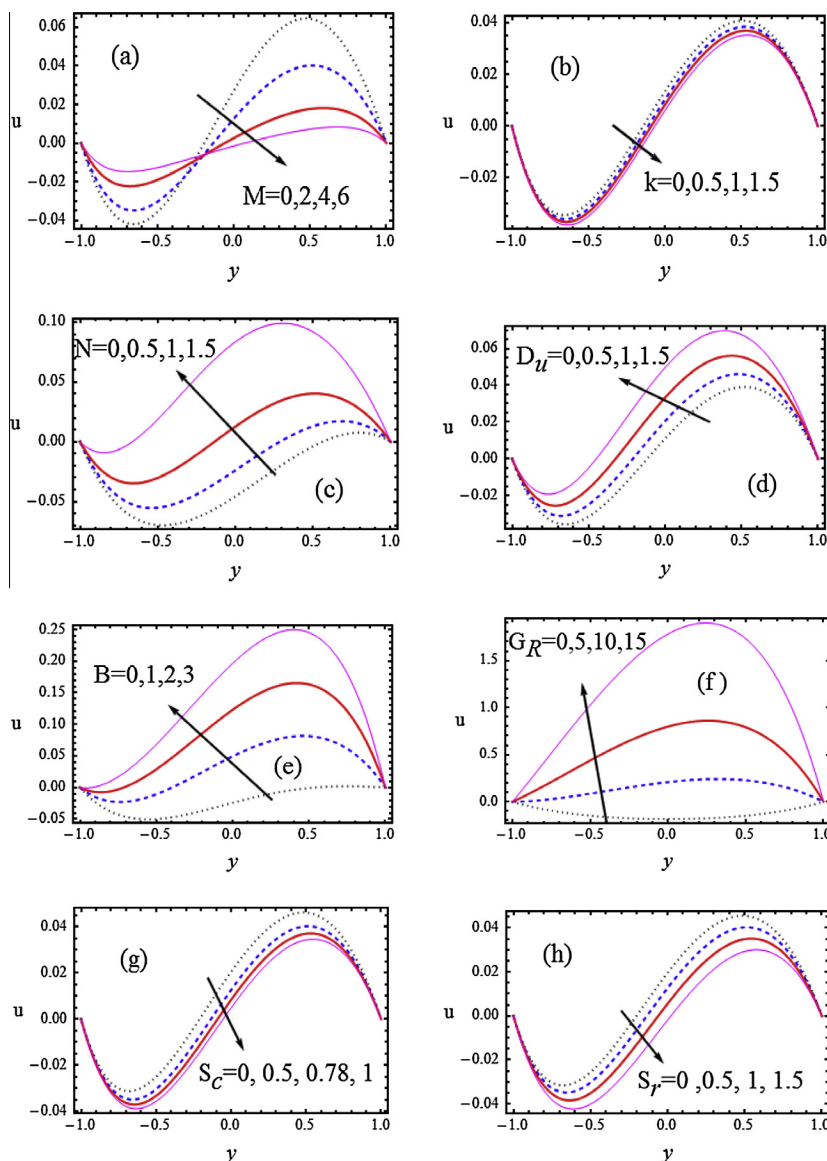


**Figure 3** Velocity distribution ( $S_r = 0.5, \alpha = 1, P_r = 0.71, \beta_1 = 0.5, N_t = 1, M = 2, S_c = 0.5, k = 0.1, N = 1, B = 0.5, D_u = 0.1$ ).

According to Fig. 2, the convergence ranges of  $u'(0)$ ,  $\theta'(0)$ ,  $\phi'(0)$  are variable for different values of parameters. In addition to the convergence, the accuracy of HAM solutions is calculated through the residual error of Eqs. (8)–(10) in the following way:

$$E_1 = \frac{d^2 u}{dy^2} + \frac{G_r}{R_c} [\theta + B\phi] - M^2 u - \alpha \quad (40)$$

$$E_2 = \frac{d^2 \theta}{dy^2} + D_u P_r \frac{d^2 \phi}{dy^2} + N\theta \quad (41)$$

$$E_3 = (N_t + \theta)^2 \frac{d^2 \phi}{dy^2} + S_r S_c (N_t + \theta)^2 \frac{d^2 \theta}{dy^2} + k S_c (N_t + \theta) \frac{d\theta}{dy} \frac{d\phi}{dy} + \left[ S_c k (N_t + \theta) \frac{d^2 \theta}{dy^2} - S_c k \left( \frac{d\theta}{dy} \right)^2 \right] (\phi + \beta_1) \quad (42)$$

where  $E_1$ ,  $E_2$  and  $E_3$  correspond to the residual error at  $m$ th order for  $u$ ,  $\theta$  and  $\phi$ , respectively. The average square residual error  $\Delta_m$  at  $m$ th order is as follows:

$$\Delta_m = \frac{1}{3} \sum_{i=1}^3 \int_{y=-1}^{y=1} E_i^2 dy \quad (43)$$

It is clear that Eq. (43) is a function of  $h$  alone and an optimal choice of the convergence control parameter is chosen in such a way that the averaged square residual error is minimum. Furthermore, the validity for the choice of the optimal value of  $h$  is confirmed because there is a good agreement between the analytical and the numerical solutions (See Fig. 9). The numerical solution is obtained by NDSolve scheme of Mathematica. Table 1 shows the square residual error and the average square residual error at 5th, 10th and 15th order of HAM approximation for different set of parameter values with optimal  $h$ . We note that this optimal value of  $h$  which is obtained after the minimization of the

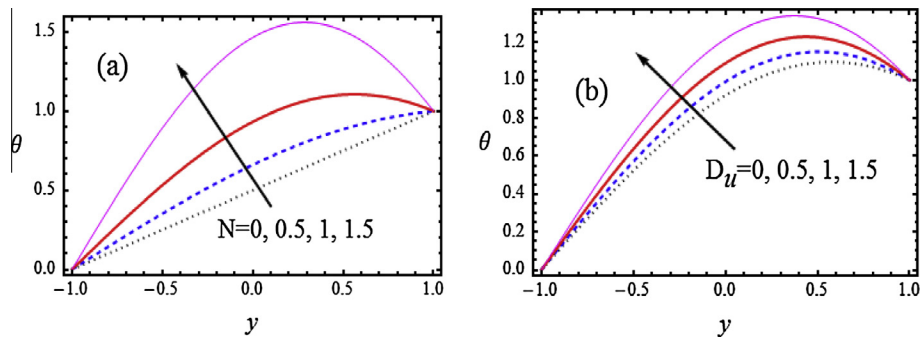


**Figure 4** Temperature distribution ( $S_r = 0.5, G_R = 1, M = 2, \alpha = 1, P_r = 0.71, \beta_1 = 0.5, N_t = 1, N = 1, B = 0.5, D_u = 0.1, S_c = 0.5, k = 0.1$ ).

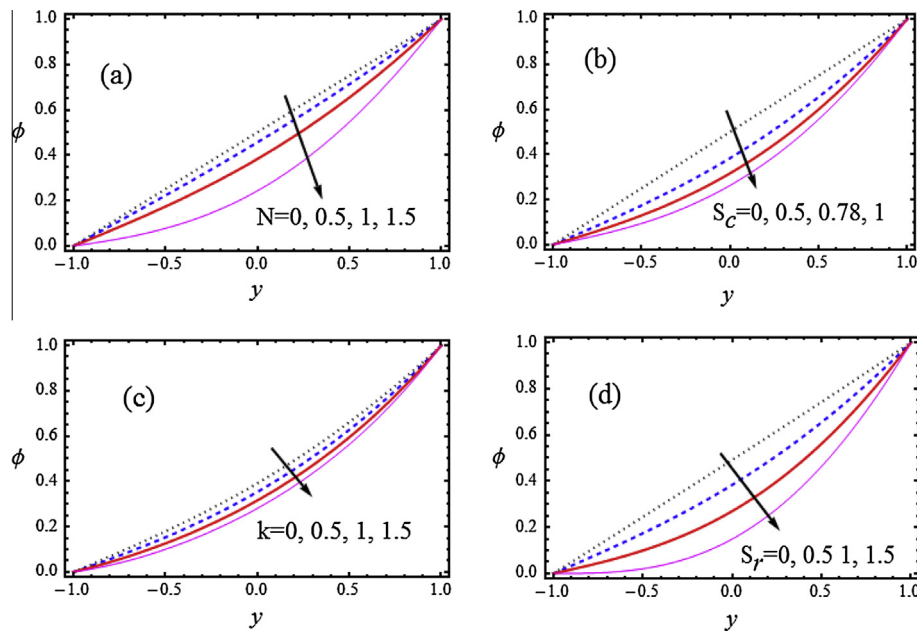


**Figure 5** Concentration distribution ( $S_r = 0.5, G_R = 1, M = 2, \alpha = 1, P_r = 0.71, \beta_1 = 0.5, N_t = 1, B = 0.5, S_c = 0.5, D_u = 0.1, N = 1, k = 0.5$ ).

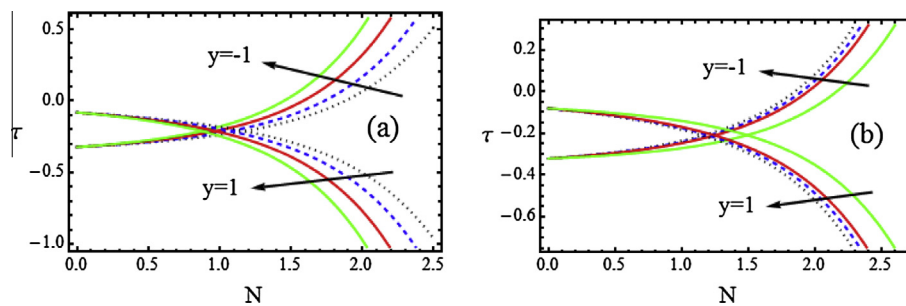


**Figure 6** Skin friction distribution ( $S_r = 0.5, G_R = 1, M = 2, \alpha = 1, P_r = 0.71, \beta_1 = 0.5, N_t = 1, B = 0.5, D_u = 0.1, k = 0.5, N = 1$ ) (a) ...  $D_u = 0$ , ...  $D_u = 0.5$ , ...  $D_u = 1$ , ...  $D_u = 1.5$  and (b) ...  $S_c = 0.5$ , ...  $S_c = 0.78$ , ...  $S_c = 1$ , ...  $S_c = 2$ .

average residual error belongs to the region of convergence found by  $h$ -curves. We observe from this table that increasing order of HAM approximation leads to more accurate

solutions. We find that the 15th order HAM solutions are good approximations for understanding the physics of the considered problem.

5. Results and discussions

In this section, the influences of different involved parameters on the flow, heat and mass transfer characteristics have been shown graphically. The graphs are drawn by taking the value of the auxiliary parameter ‘ $h$ ’, at which the average residual error is minimum. The results presented in Fig. 3 indicate the behavior of  $M, k, N, D_u, B, G_R, S_c$  and  $S_r$  on the velocity of the fluid. The variation of the magnetic parameter ( $M$ ) is shown in Fig. 3a. This figure indicates that by increasing ‘ $M$ ’, velocity decreases in the right half of the channel but the reverse trend can be noticed in the left half of the channel. Moreover, magnitude of the velocity is a decreasing function of  $M$ . The physical explanation for the above trends is, when the transverse magnetic field is applied in a fluid introduces a damping effect on the velocity field by creating a drag force. This resistive force causes the velocity to decrease with an increase in the magnetic field parameter (as noted in Ref. [21]). Fig. 3b elucidates the effect of non-dimensional thermophoretic coefficient on  $u$ . Obviously the velocity is a decreasing function of ‘ $k$ ’ (as noted in Ref. [18]). The influence of the radiation parameter ‘ $N$ ’ is sketched in Fig. 3c. It shows that the velocity of the fluid enhances significantly which may be due to the temperature variation in the fluid. Similar effect can be noticed if the parameter ‘ $N$ ’ is replaced by ‘ $D_u$ ’, which is shown in Fig. 3d. Fig. 3e elucidates the effect of buoyancy parameter ‘ $B$ ’ on the velocity ‘ $u$ ’. It is observed that increasing ‘ $B$ ’ enhances the velocity field because of increase in the buoyancy ratio that tends to increase the buoyancy-induced flow. Fig. 3f has been plotted to illustrate the variations of mixed convection parameter ( $G_R$ ) on main velocity  $u$ . It is found that

the effect of increasing  $G_R$  is to increase the velocity as expected. An increasing  $G_R$  physically means an increase of the buoyancy force, which supports the flow. Further, It is apparent from Fig. 3g that the velocity is a decreasing function of  $S_c$ . Similar effect could be noticed with increasing  $S_r$ , which is shown in Fig. 3h.

Fig. 4 is plotted to illustrate the variations of  $N$  and  $D_u$  on the temperature distribution. Fig. 4a elucidates the effects of  $N$  on  $\theta$ . It is found that increasing  $N$  leads to increase the fluid temperature. Fig. 4b gives the behavior of  $D_u$  on  $\theta$ . It is noted that  $D_u$  has similar results when compared with Fig. 4a. But the change in Fig. 4b is smaller when compared with Fig. 4a. Fig. 5 is made to see the variation of  $\phi$  versus  $y$  with different values of  $N, S_c, k$  and  $S_r$ . Similar observations are gathered from these figures, which shows that increasing these values suppresses the concentration of the fluid. It is important to note that,  $\phi$  is monotonically decreasing function of  $y$  in the left half of the channel (See Ref. [16]). Fig. 6 is plotted for skin friction against the radiation parameter. From Fig. 6a, we observe that the skin friction is increased with an increase of ‘ $N$ ’ at  $y = -1$  while it decreases at the other wall. The effect of  $D_u$  on  $\tau$  is same on both the walls. The influence of  $S_c$  on  $\tau$  is sketched in Fig. 6b. It depicts that the opposite result to that of Fig. 6a if  $D_u$  is replaced by  $S_c$ . To see the behavior of Nusselt number distribution for different values of  $D_u$  and  $S_c$ , we have prepared Fig. 7. The influence of both the parameters on Nu is just opposite to that of Fig. 6a, which is shown in 7a&7b. The reverse effect can be observed with increasing these parameters on Sherwood distribution which is shown in Fig. 8. Proper choice of the parameters and making the boundary conditions similar to [16] for  $u$ , we note that HAM

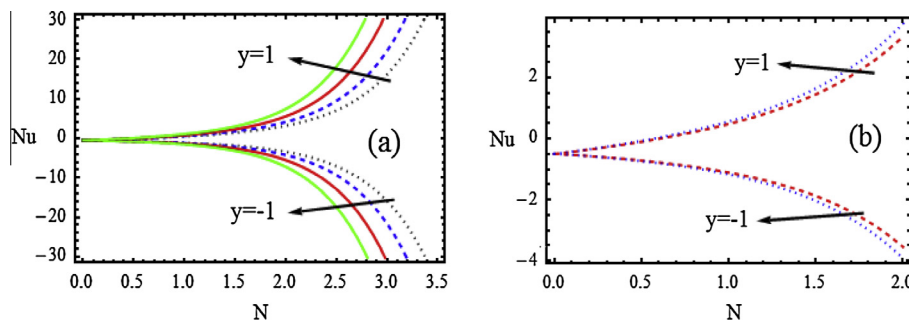


Figure 7 Nusselt number distribution ( $S_r = 0.5, G_R = 1, M = 2, \alpha = 1, P_r = 0.71, \beta_1 = 0.5, N_t = 1, B = 0.5, D_u = 0.1, k = 0.5, N = 1$ ), (a) ...  $D_u = 0$ , ...  $D_u = 0.5$ , ...  $D_u = 1$ , ...  $D_u = 1.5$  and (b) ...  $S_c = 0.5$ , ...  $S_c = 2$ .

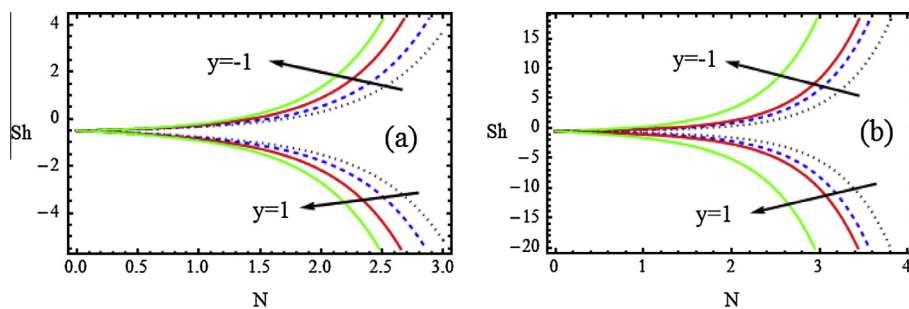
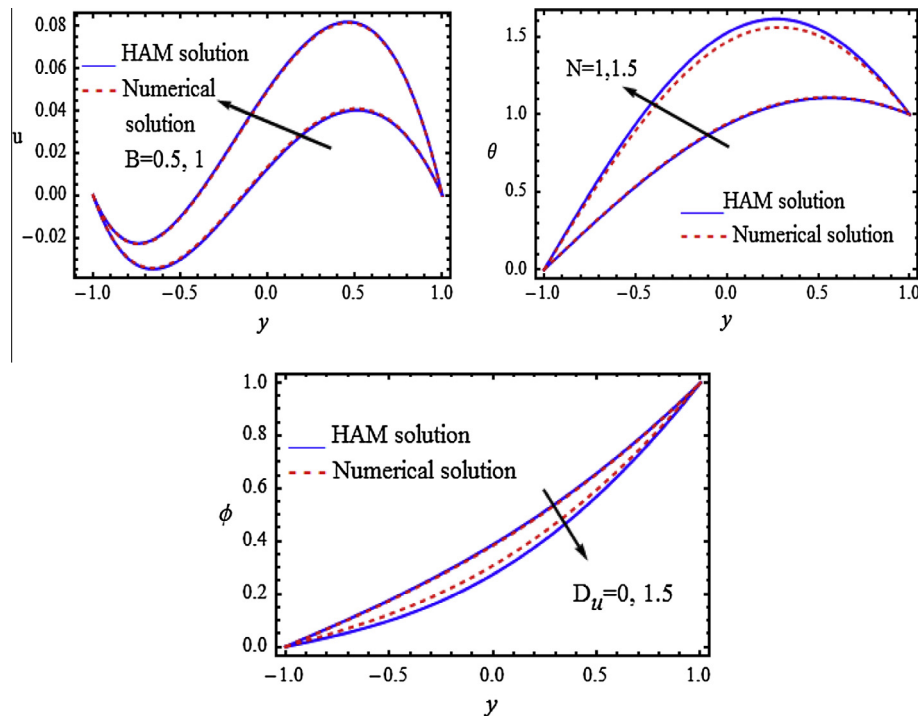
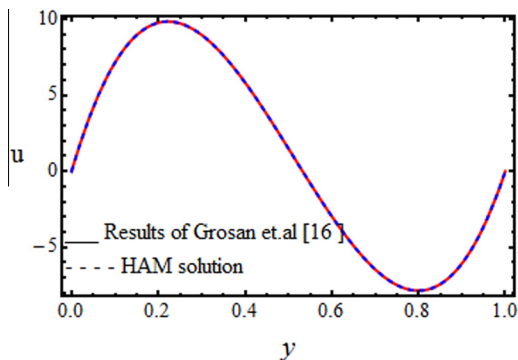


Figure 8 Sherwood number distribution ( $S_r = 0.5, G_R = 1, M = 2, \alpha = 1, P_r = 0.71, \beta_1 = 0.5, N_t = 1, B = 0.5, D_u = 0.1, k = 0.5, N = 1$ ), (a) ...  $D_u = 0$ , ...  $D_u = 0.5$ , ...  $D_u = 1$ , ...  $D_u = 1.5$  and (b) ...  $S_c = 0.5$ , ...  $S_c = 0.78$ , ...  $S_c = 1$ , ...  $S_c = 2$ .





**Figure 9** Comparison of HAM and Numerical results ( $S_r = 0.5, G_R = 1, M = 2, \alpha = 1, D_u = 0.1, P_r = 0.71, \beta_1 = 0.5, N_t = 1, B = 0.5, D_u = 0.1, S_c = 0.5, k = 0.5, N = 1$ ).



**Figure 10** Velocity distribution ( $S_r = 0, G_R = 100, M = 0, \alpha = -12, D_u = 0, P_r = 0, N_t = 1, B = 10, D_u = 0, S_c = 100, k = 0, N = 0$ ).

solutions show very good agreement with the solutions given by Grosan and Pop [16] (See Fig. 10).

## 6. Final remarks

In this article, the effects of thermophoretic particle deposition on the MHD mixed convective heat and mass transfer flow in a vertical channel in the presence of a magnetic field. The resulting nonlinear coupled equations are solved under appropriate boundary conditions using the homotopy analysis method. Particular attention is given to show graphically the variations of pertinent parameter on the flow, heat and mass transfer characteristics. It is interesting to note that the velocity is an increasing function of  $N, D_u, B$  and  $G_R$

while it decreasing function of  $M, k, S_r$  and  $S_c$ . The fluid temperature increases with increasing  $N$  and  $D_u$ . The influences of  $N, S_c, k,$  and  $S_r$  on the concentration distribution are same and  $\phi$  is decreasing function of  $y$  in the left half of the channel (See Ref. [16]). Effect of radiation parameter on Nusselt number distribution is just opposite to Sherwood distribution at the walls. Skin friction is increased with an increase of ' $N$ ' at the channel wall  $y = -1$  whereas the reverse effect is true at the other wall. The results of Grosan et al. [16] can be captured as a limiting case of  $M, D_u, P_r, N$  and  $S_r \rightarrow 0$ .

## References

- [1] Tao LN. On combined free and forced convection in channel. *ASME J Heat Transfer* 1960;82:233–8.
- [2] Aung W, Worku G. Developing flow and flow reversal in a vertical channel with symmetric wall temperatures. *ASME J Heat Transfer* 1986;108:299–304.
- [3] Cheng CH, Kou HS, Huang WH. Flow reversal and heat transfer of fully developed mixed convection in vertical channels. *J Thermophys* 1990;4:375–83.
- [4] Barletta A. Laminar mixed convection with viscous dissipation in a vertical channel. *Int J Heat Mass Transfer* 1998;41:3501–13.
- [5] Chamkha AliJ, Grosan T, Pop I. Fully developed free convection of a micropolar fluid in a vertical channel. *Int Commun Heat Mass Transfer* 2002;29:1119–27.
- [6] Srinivas S, Muthuraj R. MHD flow with slip effects and temperature-dependent heat source in a vertical wavy porous space. *Chem Eng Commun* 2010;197:1387–403.
- [7] Srinivas S, Muthuraj R. Effects of chemical reaction and space porosity on MHD mixed convective flow in a vertical asymmetric channel with peristalsis. *Math Comput Modell* 2011;54:1213–27.

- [8] Hang Xu, Pop I. Fully developed mixed convection flow in a vertical channel filled with nanofluids. *Int Commun Heat Mass Transfer* 2012;39:1086–92.
- [9] Rashidi MM, Hayat T, Erfani E, Mohimani Pour SA, Awatif A-Hendi. Simultaneous effects of partial slip and thermal-diffusion and diffusion-thermo on steady MHD convective flow due to a rotating disk. *Commun Nonlinear Sci Numer Simul* 2011;16:4303–17.
- [10] Opiolka S, Schmidt F, Fissan F. Combined effect of electrophoresis and thermophoresis on particle deposition onto flat surfaces. *J Aerosol Sci* 1994;25:665–71.
- [11] He C, Ahmadi G. Particle deposition with thermophoresis in laminar and turbulent duct flow. *Aerosol Sci Technol* 1998;29:525–46.
- [12] Garg VK, Jayaraj S. Thermophoresis of aerosol particle in laminar flow over inclined plates. *Int J Heat Mass Transfer* 1998;31:875–90.
- [13] Selim A, Hossain MA, Rees DAS. The effect of surface mass transfer on mixed convection flow past a heated vertical flat permeable plate with thermophoresis. *Int J Therm Sci* 2003;42:973–82.
- [14] Chamka A, Pop I. Effect of thermophoresis particle deposition in free convection boundary layer from a vertical flat plate embedded in a porous medium. *Int Commun Heat Mass Transfer* 2004;31:421–30.
- [15] Bakier AY, Mansour MA. Combined of magnetic field and thermophoresis particle deposition in free convection boundary layer from a vertical flat plate embedded in a porous medium. *Thermal Sci* 2007;11:65–74.
- [16] Grosan T, Pop R, Pop I. Thermophoretic deposition of particles in fully developed mixed convection flow in a parallel-plate vertical channel. *Heat Mass Transfer* 2009;45:503–9.
- [17] Magyari E. Thermophoretic deposition of particles in fully developed mixed convection flow in a parallel-plate vertical channel: the full analytical solution. *Heat Mass Transfer* 2009;45:1473–82.
- [18] Mahdy A, Hady FM. Effect of thermophoretic particle deposition in non-Newtonian free convection flow over a vertical plate with magnetic field effect. *J Non-Newton Fluid Mech* 2009;161:37–41.
- [19] Singh NP, Singh AK, Singh AK, Agnihotri P. Effects of thermophoresis on hydromagnetic mixed convection and mass transfer flow past a vertical permeable plate with variable suction and thermal radiation. *Commun Nonlinear Sci Numer Simul* 2011;16:2519–34.
- [20] Noor NFM, Abbasbandy S, Hashim I. Heat and mass transfer of thermophoretic MHD flow over an inclined radiate isothermal permeable surface in the presence of heat source/sink. *Int J Heat Mass Transf* 2012;55:2122–8.
- [21] Guha A, Samanta S. Effect of thermophoresis on the motion of aerosol particles in natural convective flow on horizontal plates. *Int J Heat Mass Transf* 2014;68:42–50.
- [22] Wang ZK, Cao TA. *An Introduction in Homotopy method*, Chongqing Publishing House Chongqing, 1991.
- [23] Liao SJ. *Beyond perturbation: introduction to homotopy analysis method*. Boca Raton Florida: Chapman & Hall/CRC Press; 2003.
- [24] Hayat T, Khan M, Asghar S. Homotopy analysis of MHD flows of an Oldroyd 8-constant fluid. *Acta Mech* 2004;168:213–31.
- [25] Hang X, Liao SJ, Pop I. Series solution of unsteady boundary layer flows of non-Newtonian fluids near a forward stagnation point. *J Non-Newtonian Fluid Mech* 2006;139:31–43.
- [26] Abdulaziz O, Noor NFM, Hashim L. Homotopy analysis method for fully developed MHD micropolar fluid flow between vertical porous plates. *Int J Numer Methods Eng* 2009;78:817–27.
- [27] Srinivas S, Muthuraj R. Effects of thermal radiation and space porosity on MHD mixed convection flow in a vertical channel using homotopy analysis method. *Commun Nonlinear Sci Numer Simul* 2010;15:2098–108.
- [28] Liao SJ. An optimal homotopy-analysis approach for strongly nonlinear differential equations. *Commun Nonlinear Sci Numer Simul* 2010;15:2003–16.
- [29] Liao SJ. *Homotopy analysis method in nonlinear differential equations*. Heidelberg: Springer & Higher Education Press; 2012.
- [30] Rashidi MM, Shooshtari A, Anwar Bég O. Homotopy perturbation study of nonlinear vibration of von Karman rectangular plates. *Comput. Struct.* 2012;106–107:46–55.
- [31] Martin O. On the homotopy analysis method for solving a particle transport equation. *Appl Math Model* 2013;37:3959–67.
- [32] Shukla AK, Ramamohan TR, Srinivas S. Analytical solutions for limit cycles of the forced Van Der Pol Duffing Oscillator. *AIP Conf Proc* 2013;1558:2187–92.
- [33] Hang Xu, Pop I. Fully developed mixed convection flow in a horizontal channel filled by a nanofluid containing both nanoparticles and gyrotactic microorganisms. *Eur J Mech B Fluids* 2014;46:37–45.
- [34] Shukla AK, Ramamohan TR, Srinivas S. A new analytical approach for limit cycles and quasi-periodic solutions for nonlinear oscillators: the example of the forced Van der Pol Duffing oscillator. *Physica Scripta* 2014;89:075202 [10pp].
- [35] Muthuraj R, Srinivas R, Shukla AK, Ramamohan TR. Effects of thermal-diffusion, diffusion-thermo, and space porosity on MHD mixed convective flow of micropolar fluid in a vertical channel with viscous dissipation. *Heat Transfer – Asian Research* 2014;43:561–76.



**D. Lourdu Immaculate** is an Assistant Professor in the Department of Mathematics, The American College, Madurai. She obtained her M.Phil in School of Mathematics, Madurai Kamaraj University, Madurai. She pursuing her PhD at Bharathiyar University, Coimbatore.



**Dr. R. Muthuraj** obtained his PhD from the VIT University, Vellore. He has research interest in Newtonian/non-Newtonian flows in channels with heat and mass transfer effects. He has published 19 research papers in refereed journal. Presently, he is a Professor of Mathematics in PSNA college of engineering and Technology, Dindigul-624622, Tamil nadu, India.



**Mrs. R.K. Selvi** obtained her M.Phil from the School of Mathematics, Madurai Kamaraj University, Madurai. Presently, she is working as an Assistant Professor in PSNA college of Engineering and Technology, Dindigul. She pursuing her PhD at Bharathiyar University, Coimbatore.



**S. Srinivas** obtained his Doctoral Degree from NIT(formerly REC), Warangal, India. He has about 25 years of teaching and research experience. He has research interest in MHD flows, Heat and Mass Transfer, Boundary layer flows, Non-Newtonian flows, Nanofluids He has published 80 research papers in various journals and conference proceedings. The total citations of his papers, as per Google Scholar, exceeds 1100. He is a reviewer for

several international journals. Presently he is a Senior Professor in the Fluid Dynamics Division of School of Advanced Sciences at VIT University, Vellore, India.



**Anant Kant Shukla** is an Assistant Professor at Department of Mathematics, Amrita Vishwa Vidyapeetham, Amrita School of Engineering, Coimbatore, India. He has submitted his PhD thesis at VIT University, Vellore, India. He was Research Scholar at CSIR Fourth Paradigm Institute (Formerly, CSIR-CMMACS), Bangalore during his PhD tenure. His current research interests are nonlinear dynamics and fluid dynamics. He has published 8 research papers in refereed journals.